Bioorganic & Medicinal Chemistry xxx (xxxx) xxx–xxx

Contents lists available at ScienceDirect

Bioorganic & Medicinal Chemistry

journal homepage: www.elsevier.com/locate/bmc

Dimeric cinnamoylamide analogues for regulation of tyrosinase activity in melanoma cells: A role of diamide-link chain length

Ji hoon Ha, Soo Nam Park*

Department of Fine Chemistry, Cosmetic R&D Center, Seoul National University of Science and Technology, 232 Gongneungro, Nowon-gu, Seoul 01811, Republic of Korea

ARTICLE INFO

Keywords:
Dimeric compound
Cinnamoyl analogues
Depigementing activity
Diamide-link chain length
Density functional theory

ABSTRACT

Dimeric cynnamoyl analogues (DCAs) with depigmenting activity have been developed. In this study, a role of diamide linkage chain length of DCAs as a tyrosinase inhibitor was investigated on tyrosinase inhibitory activity, antioxidative activity, hydrophobicity and anti-melanogenesis as well as structural characteristics and dipole moments based on density functional theory. DCAs with different diamide-link chain lengths (n = 2, 3, and 4) and various functional groups (*m*-coumaroyl, *p*-coumaroyl, isoferuloyl and feruloyl groups) were synthesized. DCAs with a diamide-link chain length of three indicated high inhibitory effect of melanin production on α-melanocyte stimulating hormone (α-MSH) stimulated B16F1 cells. Approach of *p*-hydroxyl group of DCAs to active site of tyrosinase, an important melanogenic enzyme, is interfered by addition of *m*-methoxy group. In structural modeling based on density functional theory, DCAs with a diamide-link chain length of three showed folded shapes, and they had lower dipole moment than with a diamide-link chain length of two or four. Thus, for the enhancement of the depigmenting activities of dimeric compounds, the diamide-link chain length is important. Our results provide an important index for the design of dimeric compounds with physiological activities.

1. Introduction

The skin color of a person depends on the distribution of blood vessels, thickness of stratum corneum, and various components such as melanin, carotene, and hemoglobin.[1,2] Melanin, which is responsible for the dark color of the skin, is a lipophilic natural polymer. Melanin is produced by a defense mechanism to protect the skin against ultraviolet radiation. However, excessive production and accumulation of melanin causes aesthetic problems, such as freckles and melasma, by hyperpigmentation in melanocytes.[3–6]

Melanin is biosynthesized in melanocytes distributed in the basal layer of the skin epidermis, then transferred to the keratinocytes.[6–8] Copper-containing tyrosinase is a major enzyme involved in melanin synthesis. Tyrosinase is an important rate-controlling step in melanin biosynthesis through the catalysis of two distinct reactions: hydroxylation of L-tyrosinase to L-DOPA, and the subsequent oxidation of L-DOPA to DOPA quinone.[9,10]

Ultraviolet rays damage the skin both directly and indirectly, resulting in the acceleration of skin aging characteristics such as wrinkle formation and pigmentation. In particular, the increase of reactive oxygen species (ROS) stimulates the keratinocytes of the epidermis to promote melanin production in melanocytes through the secretion of compounds such as NO and α-melanocyte stimulating hormone (α-MSH).[11] In addition, free iron released after cell damage produces ROS such as the hydroxyl radical (·OH) through the Fenton reaction with hydrogen peroxide, which promotes oxidation of the melanin precursor and melanin production.[12] Therefore, antioxidative activity is very important for inhibiting melanogenesis as well as the inhibitory activity of tyrosinase.

L-Ascorbic acid, *p*-coumaric acid, and ferulic acid are known to inhibit the activity of tyrosinase through antioxidative activity and blocking the active sites of tyrosinase.[13–15,16] L-Ascorbic acid decreases melanin production by supplying hydrogen to oxidized DOPA quinone, resulting in the restoration of DOPA quinone to DOPA.[17]

Strong inhibitors of tyrosinase such as hydroquinone, kojic acid, and arbutin, act as competitive inhibitors that bind to the active site of tyrosinase owing to their similar structure to tyrosine.[18,19] However, rhododendrol, known as a potential tyrosinase inhibitor, causes an

Abbreviations: DCAs, dimeric cinnamoylamide analogues; α-MSH, α-melanocyte stimulating hormone; ROS, reactive oxygen species; DFP, *N,N′*-diferuloyl-putrescine; DPPH radical, 1,1-diphenyl-2 picrylhydrazyl radical

* Corresponding author: Department of Fine Chemistry, Cosmetic R&D Center, Cosmetic Industry Coupled Collaboration Center, Seoul National University of Science and Technology, 232 Gongneung-ro, Nowon-gu, Seoul 01811, Republic of Korea.
E-mail address: snpark@seoultech.ac.kr (S.N. Park).

https://doi.org/10.1016/j.bmc.2018.10.036
Received 22 August 2018; Received in revised form 20 October 2018; Accepted 29 October 2018

acute problem on the skin.[20,21] Therefore, development of a safe whitening material is required.[22]

Dimeric cinnamoylamide analogues (DCAs) as depigmenting agents were isolated from Sophora japonica L. and corn bran[23,24] and synthesized to enhance depigmenting activity. In particular, DCAs with different cinnamoyl derivatives and a diaminoethyl group.[25] Kim et al.[26] synthesized DCAs containing hydroxyl groups at various positions and different diamide-link chain lengths. However, the role of diamide-link chain lengths on DCAs with hydroxymethoxyl group was not reported for depigmenting activity.

In this study, DCAs with cinnamoyl derivatives (feruloyl, isoferuloyl, p-coumaroyl or m-coumaroyl) and different diamide-link chain lengths (n = 2, 3, or 4) were synthesized and evaluated on tyrosinase and melanogenesis inhibitory effect. Our results provide useful information about structure-activity relationship of DCAs for depigmenting activities.

2. Experimental section

2.1. Chemistry

2.1.1. Instruments and chemicals

The UV-VIS spectrophotometer used in this study was a Varian (Australia) Cary 50, a Spectronic 20D system (Milton Roy Co., USA) was used to measure the cellular protective effect. A Berthold (Germany) 6-channel LB9505 LT system was used for the chemiluminescence assay, and the nuclear magnetic resonance (NMR) spectrometer used here was a 400 MHz NMR system (Varian Inc., USA). Na_2HPO_4, NaH_2PO_4, ethylenediaminetetraacetic acid (EDTA), H_2O_2, luminol and heparin were purchased from Sigma Chemical Co. (St. Louis, MO). $FeCl_3{\cdot}6H_2O$ was bought from Junsei Chemical Co. (Japan). Ethanol (EtOH), methanol (MeOH), ethyl acetate (EtOAc), and acetonitrile were purchased from as the highest purity and HPLC grade from Sigma Chemical Co. (St. Louis, MO). Dulbecco's modified Eagle's medium (DMEM), fetal bovine serum (FBS), and penicillin-streptomycin, and bovine serum albumin (BSA) were obtained from PAA Co. (Pasching, Austria).

2.1.2. Physicochemical characteristics of dimeric cinnamoylamide analogues

N,N'-di-m-coumaroyl-1,2-diaminoethane (**1**): White power, Yield 51.8%, λmax (278 nm), HRMS (EI+): *m/z*: calcd for C20H20N2O4: 353.14, ^{1}H NMR(400 MHz, DMSO-d_6): 3.28(4H, d), 6.55(2H, d, J = 15.4), 6.79–6.77(2H, m, J = 2), 6.93(2H, s), 6.97–6.93(2H, m, J = 6.6), 7.22–7.19(2H, t, J = 7.7), 7.53(2H, d, J = 16.1), 8.26(2H, t, J = 5.6), 9.59(2H, s). ^{13}C NMR (DMSO-d_6): 164.7, 157.1, 138.4, 135.6, 129.3, 121.3, 118.1, 116.1, 113.1, 24.5.

N,N'-di-m-coumaroyl-1,3-diaminopropane (**2**): White power, Yield 75.7%, λ_{max} (280 nm), HRMS (EI+): *m/z*: calcd for C21H22N2O4: 366.16, ^{1}H NMR(400 MHz, DMSO-d_6): 1.69–1.66(2H, m, J = 7.0), 3.24–3.21(2H, d, J = 7.0), 6.56–6.54(2H, d, J = 15.4), 6.79–6.76(2H, m, J = 1.4), 6.94(2H, t, J = 2.1), 6.99(2H, d, J = 7.7), 7.21(2H, t, J = 7.7), 7.34(2H, d, J = 15.4, 8.16(2H, t, J = 5.6), 6.99(2H, d, J = 7.7), 7.21(2H, t, J = 7.7), 7.34(2H, d, J = 15.4), 8.16(2H, t, J = 5.6), 9.59(2H, s). ^{13}C NMR (DMSO-d_6): 164.4, 157.0, 138.2, 135.6, 129.3, 121.4, 118.1, 116.0, 113.0, 36.6, 28.7.

N,N'-di-m-coumaroyl-1,4-diaminobutane (**3**): White power, Yield 61.4%, λ_{max} (278 nm), HRMS (EI+): *m/z*: calcd for C22H24N2O4: 381.17, ^{1}H NMR(400 MHz, DMSO-d_6): 1.49(4H, s), 3.20(4H, d, J = 5.20), 6.54(2H, d, J = 9.6), 6.79–6.76(2H, dd, J = 2.0), 6.92(2H, s), 6.98(2H, d, J = 7.6), 7.18(2H, t, J = 7.6), 7.34(2H, d, J = 15.6), 8.14(2H, t, J = 5.2), 9.59(2H, s). ^{13}C NMR (DMSO-d_6): 164.8, 157.7, 157.6, 138.6, 129.8, 121.9, 118.4, 116.6, 113.6, 38.3, 26.7.

N,N'-di-p-coumaroyl-1,2-diaminoethane (**4**): White power, Yield 59.2%, λ_{max} (310 nm), HRMS (EI+): *m/z*: calcd for C20H20N2O4: 353.14, 1H NMR(400 MHz, DMSO-d_6): 3.27(4H, d), 6.42(2H, s), 6.80(4H, d, J = 8.40), 7.36(2H, d, J = 15.6), 7.40(4H, d, J = 8.8), 8.12(2H, s), 9.85(2H, s).^{13}C NMR (DMSO-d_6): 166.1, 159.3, 139.2, 129.7, 126.3, 119.0, 116.2, 39.1.

N,N'-di-p-coumaroyl-1,3-diaminopropane (**5**): White power, Yield 79.9%, λ_{max} (310 nm), HRMS (EI+): *m/z*: calcd for C21H22N2O4: 367.16, ^{1}H NMR(400 MHz, DMSO-d_6): 1.63(2H, t, J = 7.0), 3.21–3.18(4H, m, J = 7.0), 6.41(2H, d, J = 15.4), 6.79–6.78(4H, m, J = 2.1), 7.33(2H, d, J = 16.1), 7.40–7.38(2H, m, J = 5.6), 9.84(2H, s). ^{13}C NMR (DMSO-d_6): 164.8, 158.2, 138.0, 128.6, 125.6, 125.3, 118.0, 115.1, 35.9, 28.8.

N,N'-di-p-coumaroyl-1,4-diaminobutane (**6**): White power, Yield 60.9%, λ_{max} (309 nm), HRMS (EI+): *m/z*: calcd for C22H24N2O4: 381.17, ^{1}H NMR(400 MHz, DMSO-d_6): 1.47(4H, s), 3.02(4H, t, J = 6.0), 6.42(2H, d, 15.6), 6.79(4H, d, J = 8.4), 7.34(2H, d, J = 16), 7.39(4H, d, J = 8.8), 8.01(2H, t, J = 5.6) 9.83(2H, s).^{13}C NMR (DMSO-d_6): 165.8, 148.7, 148.3, 139.3, 126.9, 121.3, 119.5, 116.1, 111.1, 55.9, 38.8, 27.3.

N,N'-diisoferuloyl-1,2-diaminoethane (**7**): White power, Yield 64.2%, λ_{max} (320 nm), HRMS (EI+): *m/z*: calcd for C22H24N2O6: 413.16, ^{1}H NMR(400 MHz, DMSO-d_6): 3.28(4H, d), 3.79(6H, s), 6.40(2H, d, J = 16.0), 6.99–6.92(6H, m, J = 8.8), 7.13(2H, d, J = 15.6), 8.18(2H, s), 9.20(2H, s). ^{13}C NMR(DMSO-d_6): 165.9, 149.6, 139.3, 128.2, 120.8, 119.9, 113.7, 112.5, 55.0.

N,N'-diisoferuloyl-1,3-diaminopropane (**8**): White power, Yield 66.5%, λ_{max} (322 nm), HRMS (EI+): *m/z*: calcd for C23H26N2O6: 427.18, ^{1}H NMR(400 MHz, DMSO-d_6): 1.68–1.64(2H, m, J = 6.8), 3.23–3.19(4H, m, J = 6.4), 6.44(2H, d, J = 15.6), 7.01(6H, m, J = 1.6), 7.30(2H, d, J = 16), 8.14(2H, s), 8.14(2H, s), 9.25(2H, s). ^{13}C NMR(DMSO-d_6): 164.7, 148.6, 146.1, 138.1, 127.0, 119.7, 118.9, 112.7, 111.4, 54.9, 36.0, 35.9, 28.8

N,N'-diisoferuloyl-1,4-diaminobutane (**9**): White power, Yield 66.1%, λ_{max} (321 nm), HRMS (EI+): *m/z*: calcd for C24H28N2O6: 441.19, ^{1}H NMR(400 MHz, DMSO-d_6): 1.47(4H, s), 3.19(4H, d, J = 5.2), 3.79(6H, s), 6.40(2H, d, J = 12.4), 6.91(2H, d, J = 12.4), 6.98(6H, m, J = 2.0), 7.28(2H, d, J = 15.6), 8.03(2H, t, J = 5.6), 9.20(2H, s). ^{13}C NMR (DMSO-d_6): 165.6, 149.6, 147.1, 139.0, 128.3, 120.7, 113.7, 112.5, 56.0, 38.8, 27.3.

N,N'-diferuloyl-1,2-diaminoethane (**10**): White power. Yield 64.5%, λ_{max} (321 nm), HRMS (EI+): *m/z*: calcd for C22H24N2O6: 413.16, ^{1}H NMR(400 MHz, DMSO-d_6): 3.28(4H, t, J = 2.0), 3.80(6H, s), 6.46(2H, d, J = 15.6), 6.80(2H, d, J = 8.0), 7.00(2H, t, J = 1.6), 7.13(2H, d, J = 1.6), 7.36(2H, d, J = 15.6), 8.09(2H, s), 9.46(2H, s). ^{13}C NMR (DMSO-d_6): 166.1, 148.7, 148.3, 139.6, 126.8, 122.0, 119.3, 116.1, 111.2, 55.9

N,N'-diferuloyl-1,3-diaminopropane (**11**): White power. Yield 66.5%, λ_{max} (320 nm), HRMS (EI+): *m/z*: calcd for C23H26N2O6: 427.18, ^{1}H NMR(400 MHz, DMSO-d_6): 1.65(2H,t, J = 6.8), 3.21(4H, m, J = 6.8), 6.47(2H, d, J = 16), 6.80(2H, d, J = 8.40), 7.00–6.98(2H, dd, J = 1.6), 7.13(2H, d, J = 1.6), 7.34(2H, d, J = 15.6), 8.01(2H, t, J = 5.6), 9.44(2H, s). ^{13}C NMR (DMSO-d_6):164.7, 148.6, 146.1, 138.1, 127.0, 119.7, 118.9, 112.7, 111.4, 54.9, 36.0, 35.9, 28.8

N,N'-diferuloyl-1,4-diaminobutane (**12**): White power. Yield 66.5%, λ_{max} (328 nm), HRMS (EI+): *m/z*: calcd for C24H28N2O6: 441.19, ^{1}H NMR(400 MHz, DMSO-d_6): 1.47(4H, s), 3.18(4H, d, J = 4.8), 3.80(6H, s), 6.47(2H, d, J = 15.6), 6.80(2H, d, J = 8.4), 6.99(2H, t, J = 2.0), 7.12(1H, d, J = 1.60), 7.34(2H, d, J = 18.4), 8.01(2H. t, J = 5.6), 9.45(2H, s). ^{13}C NMR (DMSO-d_6): 165.7, 148.6, 148.2, 139.3, 126.9, 121.9, 119.5, 116.1, 111.1, 55.9, 38.8, 27.3.

2.2. Biological activity

2.2.1. Cell culture

B16F1 cells were gained from Korean Cell Line Bank (Seoul, Korea)[22] and were cultured in Dulbecco's modified Eagle's medium (DMEM; Capricorn, Germany) supplemented with 10% fetal bovine serum (FBS; Capricorn, Germany) and 1% penicillin/streptomycin in a humidified atmosphere containing 5% CO_2 at 37 °C.

2.2.2. Measurement of cell viability

Cell viability assay was performed using 3-(4,5-cimethylthiazol-2-yl)-2,5-diphenyl tetrazolium bromide (MTT) by measuring the reduction value of MTT to formazan. B16F1 cells were seeded at a density of 1×10^4 cells/well in a 96-well plates. Then, cells were treated indicated concentration of compounds. After incubation for 72 h, the medium was removed and washed, and MTT solution (200 μL) was added to each well. After cells were treated for 1 h, the media is removed and added DMSO for solubilization of formazan. Then, absorbance was measured using a microplate reader (TECAN, Salzburg, Austria) at 570 nm.

2.2.3. Measurement of melanin content

B16F1 cells were seeded at 1×10^5 cells/well in 6-well culture plates.[27] Then, cells were treated with indicated concentration of MAHDP for 72 h. B16F1 cells were stimulated with 200 nM α-MSH together. To analyze intracellular melanin content, cells were washed twice with PBS and dissolved in 1 N NaOH solution containing 10% DMSO at 80 °C for 2 h. The cell lysates was transferred to a new 96 well plate and determined by estimating the absorbance at 405 nm using a microplate reader.

2.2.4. Intracellular TYR inhibitory activity

To obtain intracellular TYR, B16F1 cells were harvested and lysed by stripper with RIPA buffer (cell lysis buffer). The cell lysates centrifuged at 13,000 rpm for 30 min at 4 °C and supernatant was collected. The protein concentrations in lysates were evaluated using the BCA protein assay kit (Pierce, Biotechnology, Rockford, IL, USA). Then, the lysate containing the same amount of protein (60 μg) was placed in a 96-well plate and treated with L-DOPA (10 mM), 0.1 M phosphate buffer (pH 6.5), sample solution or arbutin for 30 min at 37 °C. The absorbance was measured at 490 nm using a microplate reader.

2.3. DPPH radical scavenging activity

Free radical scavenging activity was conducted by 1,1-diphenyl-2-picryl hydrazyl (DPPH), which is used because it has a stable free radical. Various concentrations of 0.3 mL the samples were mixed with 0.3 mL 0.2 mM DPPH and 0.3 mL 100% EtOH and incubated for 10 min. The levels of free radicals was measured by absorbance at 517 nm (λ_{max} of DPPH).[24] Results were expressed as concentration of sample necessary to give a 50% reduction in the original absorbance (EC_{50}). The free radical scavenging activity was calculated using the following Eq. (1):

$$\text{Radicalscavenging\%} = \left\{1\text{-}\left(\frac{A_{Experiment} - A_{Blank}}{A_{Control}}\right)\right\} \times 100 \quad (1)$$

2.4. Determination of chelating activity

To evaluate the ability of DCAs to chelate copper, the UV–visible spectra (220–400 nm) of DCAs and

Cu-complexed counterparts were measured by the modified method.[28] The mixture, consisting of 50 μL of DCAs (50 μM) ethanol solution and 0.95 mL of the aqueous solution of $CuSO_4$ (10 μM) or water (control) was incubated at 25 °C for 10 min before UV-Vis spectral analysis. All tests and analyses were carried out in triplicate and displayed representative spectra.

3. Results and discussion

3.1. Chemistry

The synthesis of DCAs with m-coumaric acid (**1–3**), p-coumaric acid (**4–6**), isoferuloyl acid (**7–9**), feruloyl acid (**10–12**) was performed by Samkyung costech Co. In addition, 1,2-diaminoethane (**1,4,7,10**), 1,3-diaminopropane (**2,5,8,11**) or 1,4-diaminobutane (**3,6,9,12**) was used for the synthesis of DCAs as depicted (Table 1.). Representatively, the synthetic pathway of *N,N′*-diferuloyl-1,2-diaminoethane (**10**) is displayed (Scheme 1). Ferulic acid (**a**) added to the solution including acetic anhydride and dimethylaminopyridine (DMAP) in triethylamine (Et_3N), and then acetylferulic acid (**b**) was obtained. The compound **b** was refluxed in thionyl chloride ($SOCl_2$), while reacting to ethylenediamine (636 mg, 25.4 mmol) to produce *N,N′*-acetylferuloyl-1,2-diaminoethane. Finally, N,N'-diferuloyl-1,2-diaminoethane (**10**) was obtained after hydrolysis as shown in Scheme 1.

Table 1
Substitution pattern of DCAs (1–12).

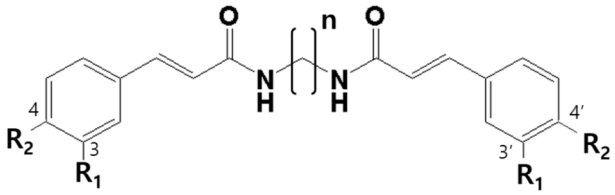

Compound	Formula	Diamide-link chain length (n)	R_1	R_2
1	C20H20N2O4	2	OH	H
2	C21H22N2O4	3	OH	H
3	C22H24N2O4	4	OH	H
4	C20H20N2O4	2	H	OH
5	C21H22N2O4	3	H	OH
6	C22H24N2O4	4	H	OH
7	C22H24N2O6	2	OH	OCH_3
8	C23H26N2O6	3	OH	OCH_3
9	C24H28N2O6	4	OH	OCH_3
10	C22H24N2O6	2	OCH_3	OH
11	C23H26N2O6	3	OCH_3	OH
12	C24H28N2O6	4	OCH_3	OH

3.2. Mushroom tyrosinase inhibitory activity

Tyrosinase inhibitory activity of DCAs is shown in Table 2, and the activity was compared to that of arbutin as positive controls.

The results indicated that the evaluated compounds present different profiles of mushroom tyrosinase inhibitory activity. Tyrosinase inhibitory activity of DCAs without hydroxy groups has been also evaluated but they did not exert any activity (data not shown).

In the experimental results, compound **3** and **10** did not exert tyrosinase inhibitory activity. Among the tested compounds, *p*-coumaroyl DCAs (**4–6**) indicated to be strong inhibitors, with IC_{50} values of 4.6, 3.4 and 6.5 μM, respectively and they showed approximately 2.3, 3.1 and 1.6 times higher active than the standard inhibitor (IC_{50} = 10.4 μM). In particular, *p*-coumaroyl DCAs showed more 16 times higher inhibitory activity than *m*-coumaroyl DCAs (**1–2**) and isoferuloyl DCAs (**7–9**) at the same amide-link chain length. These effects can be explained that *p*-hydroxybenzyl group acts as a strong competitive inhibitor because its structure is similar to the binding site of tyrosine.[29] In addition, *m*-methoxy group interferes with approaches of *p*-hydroxyl group to the active site of tyrosinase through steric hindrance.[30] Interestingly, DCAs showed high tyrosinase inhibitory activities when the diamide chain length was three (**2**, **5**, **8** and **11**). These results suggest that a methoxy group and the diamide-link chain lengths in DCAs may affect the tyrosinase inhibitory activity directly.

3.3. Antimelanogenic effects in B16F1 melanoma cells

3.3.1. Effect on cell viability

To evaluate the potential cytotoxicity of DCAs on melanoma cells, the cells were treated with different concentration of each DCAs (100,

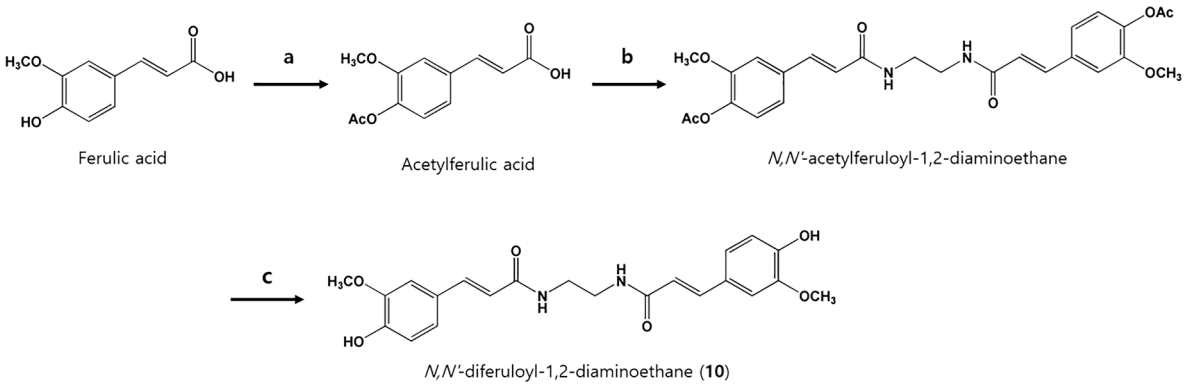

Scheme 1. Reagents and reaction conditions: (a) acetic anhydride, Et3N, DMAP (b) 1,2-diaminoethane, $SOCl_2$, Et3N, MC (c) KOH, H_2O.

Table 2
Half maximal inhibitory concentration (IC_{50}) values of DCAs against mushroom tyrosinase activity.

Compound	IC_{50} (μM)[a]
1	95.3 ± 1.2
2	55.2 ± 0.5
3	> 150
4	4.6 ± 0.04
5	3.4 ± 0.06
6	6.5 ± 0.03
7	84.2 ± 1.1
8	55.3 ± 0.1
9	80.2 ± 1.6
10	> 150
11	98.3 ± 2.1
12	108.4 ± 2.5
Arbutin[b]	10.4 ± 0.11

[a] Data represent the mean (± standard deviation, SD) of three independent experiments.
[b] Positive control.

Table 3
Effects of DCAs on tyrosinase inhibitory activity and melanin production in B16F1 cells.

Compound	IC_{50} (μM)[a]	
	Tyrosinase inhibitory activity	Melanin production
1	> 150	> 150
2	40.2 ± 1.2	95.3 ± 0.8
3	> 150	> 150
4	> 150	> 150
5	4.6 ± 0.1	45.6 ± 0.4
6	> 150	> 150
7	> 150	> 150
8	46.7 ± 1.5	111.3 ± 2.5
9	> 150	> 150
10	> 150	> 150
11	65.2 ± 1.9	122.8 ± 1.4
12	88.4 ± 3.3	> 150
Arbutin[b]	87.5 ± 3.1	148.3 ± 2.1

[a] Data represent the mean (± standard deviation, SD) of three independent experiments.
[b] Positive control.

150 and 200 μM) for 72 h and were examined using MTT assay. Results indicated that compounds **1**–**12** had no considerable cytotoxic effect in B16F1 melanoma cells at the concentration in which tyrosinase activity was inhibited (Fig. 1). Cell viabilities of compounds **1**, **3** and **6** slightly decreased at 200 μM. Therefore, the following experiments were performed using up to 150 μM of DCAs.

3.3.2. *Effect on intracellular tyrosinase activity and melanin production*

To investigate the inhibitory effect of DCAs on melanogenesis, B16F1 cells were treated with DCAs and α-MSH (200 nM), and evaluated for the concentration at which 50% of melanogenesis is suppressed (IC_{50}) (Table 3). Compounds **1**, **3**, **4**, **6**, **7**, **9** and **10** did not exert any effect (> 150 μM) on both intracellular tyrosinase activity and melanin production on α-MSH stimulated B16F1 cells. On the other hand, compounds **2**, **5**, **8**, **11** reduced melanin production, as well as intracellular tyrosinase activity. Although compounds **1**, **4**, **6**, **7**, **9** and **12** indicated inhibitory effects on mushroom tyrosinase, they didn't exert inhibitory effect on both tyrosinase activity and melanin production on α-MSH stimulated B16F1 cells. This may be due to the cellular mechanisms, not reflected in the mushroom tyrosinase screening assays.[25] Interestingly, compounds **2**, **5**, **8** and **11** with a

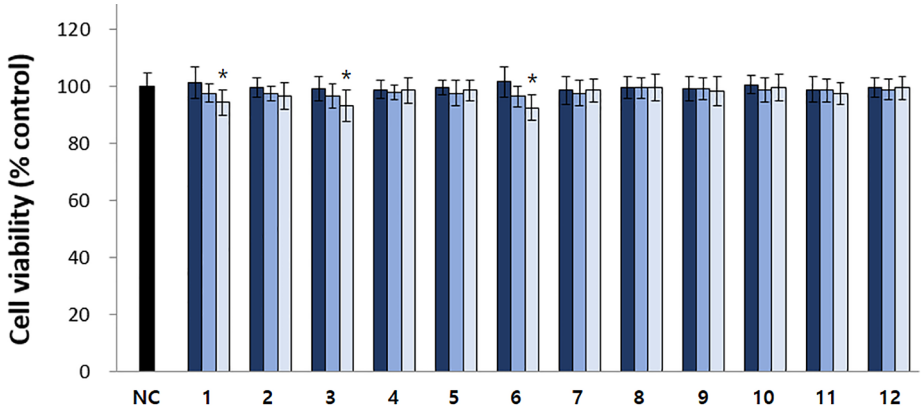

Fig. 1. Cell viability of DCAs on B16F1 cells at 100 μM (dark blue), 150 μM (cobalt blue), 200 μM (light blue). Data are presented as the mean ± SD of three independent experiments. $^{*}p < 0.01$ compared with non-treated cells (NC).

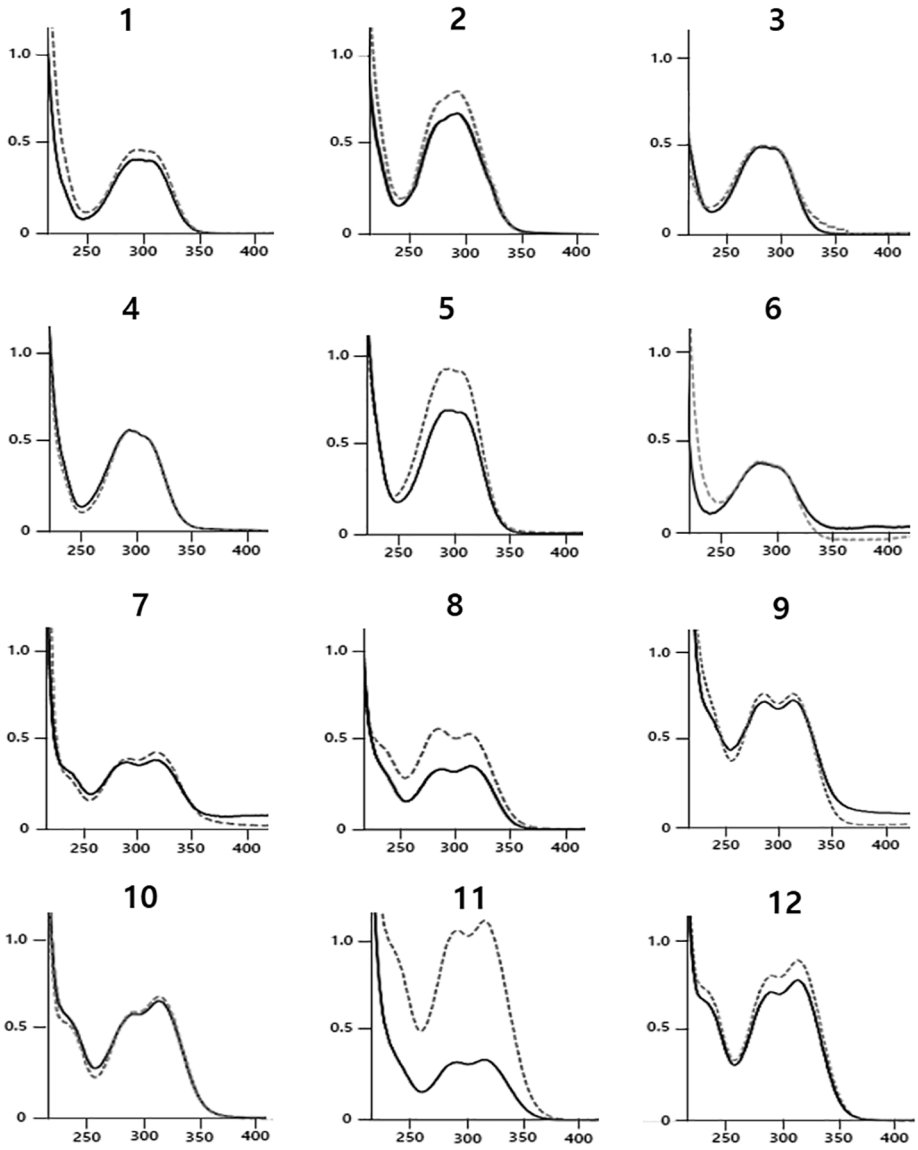

Fig. 2. Copper ions chelating ability of DCAs. The representative UV–vis spectra of compound 1–12 at 50 μM was displayed (solid line). Spectrum recorded again with the addition of 10 μM $CuSO_4$ (dotted line).

diamide-link chain length of three possessed higher inhibitory effect of tyrosinase activity and melanin production than DCAs with a diamide-link chain length of two or four. They showed more anti-melanogenesis activity than arbutin as compared with the control. Thus, the position of methoxy groups and/or hydroxyl groups in DCAs, as well as the diamide-link chain length, are important for forming the optimal structure to bind to the tyrosinase active site.

3.4. Effect on intracellular tyrosinase activity and melanin production

Tyrosinase inhibitory effects of DCAs and arbutin might be due to binding with copper as the active site of tyrosinase. The copper-chelating properties of DCAs were evaluated by spectrophotometric analyses.

As shown in Fig. 2, the max absorbance indicated widely from 280 to 320 nm for compound **1–6** with a hydroxyl group (Fig. 2, solid line). The max absorbance of compound **7–12** with hydroxyl group and methoxy group indicated two λ_{max} between 280 and 330 nm. Compound **2**, **5**, **8**, **11**, **12** showed increasing absorbance (Fig. 2, dote line) with addition of Cu (II). Interestingly, they possessed inhibitory activity on intracellular tyrosinase of B16F1 cells. There are previous studies on increase in the UV–Vis spectra of compounds with Cu (II) addition and the compounds indicated tyrosinase inhibitory activities.[27] These results suggest that melanogenesis of DCAs might be dependent on their tyrosinase inhibitory activity through copper-chelating properties.

3.5. Antioxidative activity

Free radical scavenging activity of DCAs was performed using DPPH· assay and L-ascorbic acid and arbutin were used as the positive controls.[31,32] Antioxidative activity of DCAs without hydroxy groups was also evaluated but they did not exert any activity (data not shown). Half maximal effective concentration (EC_{50}) values for the assay were indicated in Table 4.

As a results, *m*-coumaroyl (**1–3**) and *p*-coumaroyl DCAs (**4–6**) did not exert antioxidative activities in the assay. Regarding DPPH· assay, isoferuloyl (**7–9**) and feruloy DCAs (**10–12**) showed the best EC_{50} values in the same range (EC_{50} = 2.21, 2.31, 5.20, 0.09, 0.15 and 0.83 μM, respectively) as L-ascorbic acid (EC_{50} = 0.18 μM) and arbutin (EC_{50} = 1.71 μM). In particular, feruloyl DCAs (**10–12**) showed free radical scavenging activity 5–40 times higher than isoferuloyl DCAs (**7–9**) in the same rage. These effects can be explained due to the

Table 4
Free radical scavenging activities (EC_{50}) of DCAs.

Compound	EC_{50} (mM)[a]
1	> 5
2	> 5
3	> 5
4	> 5
5	> 5
6	> 5
7	2.21 ± 0.25
8	2.31 ± 0.14
9	4.20 ± 0.22
10	0.09 ± 0.001
11	0.15 ± 0.01
12	0.83 ± 0.02
L-Ascorbic acid[b]	0.18 ± 0.01
Arbutin[b]	1.7 ± 0.07

[a] Data represent the mean (± standard deviation, SD) of three independent experiments.
[b] Positive control.

Table 5
Dipole moments and partition coefficient (Log *P*) of DCAs.

Compound	Dipole moment [a]	log *P*[b]
1	7.348	2.01
2	5.975	2.12
3	6.914	2.57
4	5.543	2.01
5	5.248	2.12
6	5.279	2.57
7	8.189	1.76
8	6.199	1.86
9	7.618	2.32
10	6.747	1.76
11	6.335	1.86
12	7.054	2.32
Arbutin[b]	3.594	−0.58

[a] Debye.
[b] Log *P* (Log[octanol/water] partition coefficient) values were calculated using Chemdraw version 7.0.

presence of a methoxy group on their structures. The methoxy group as an electron-donating group enhances stabilization of the electrons produced after the transfer of hydrogen from the hydroxyl group to the free radical as DPPH.[33] Especially, *m*-methoxy group in ferulic moiety can stabilize more than *p*-methoxy group in isoferulic moiety.[34] Interestingly, compounds **7**, **8**, **10** and **11** with a diamide-link chain length of two or three were higher anti-oxidative activities than compounds **9** and **12** with a diamide-link chain length of four. Their high activities are presumed that their diamide-link chain length is important to be stabilized after electron donation.[35] These results suggest that addition and position of methoxy groups as well as length of diamide-link chain in DCAs are important to enhance antioxidative activity. Although feruloy DCAs indicated high free radical scavenging activity, they did not affect anti-melanogenesis activity.

3.6. Structure, dipole moment, log P and cell uptake

In order to study the effects of the structure and dipole moment of the DCAs in water phase, we optimized the structures of the DCAs using a Gaussian 09 W software package at the DFT level of theory (B3LYP

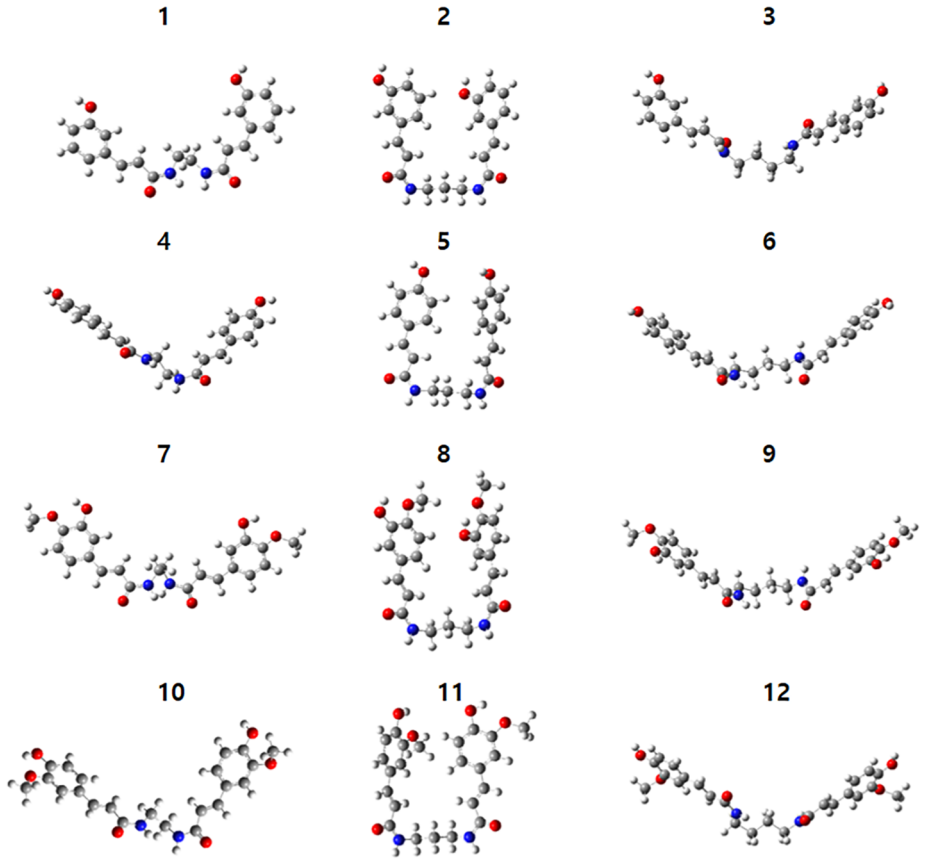

Fig. 3. DFT-optimized structures of the DCAs (**1–12**). Calculations were conducted using a Gaussian 09 W. All structure optimizations were performed by molecular-mechanics computations and were further refined by DFT computation (B3LYP at the 6-31G* level).

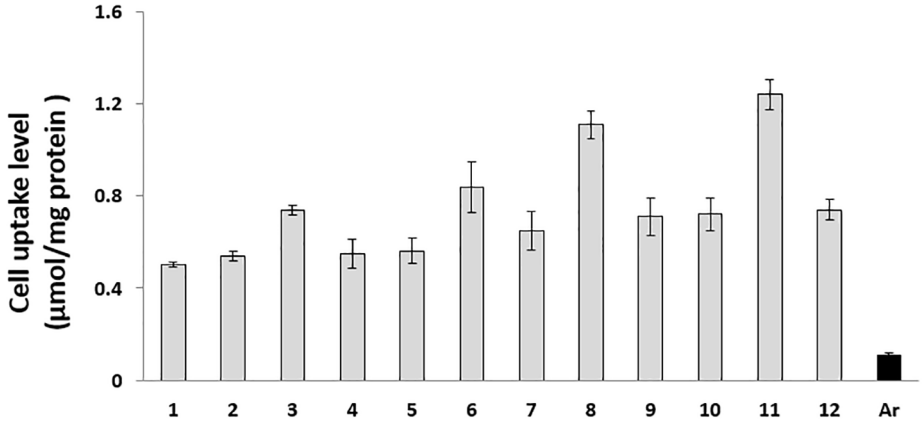

Fig. 4. Cell uptake level (μmol/mg protein) of DCAs on B16F1 cells. The cells Data are presented as the mean ± SD of three independent experiments.

hybrid functional) together with a 6-31G*(d,p) basis set in a water phase.

Compounds **2**, **5**, **8** and **11**, which are containing a diamide-link chain length of three, displayed folded structures with their functional groups pointed in the same direction (Fig. 3). The structure of them shows both hydroxyl groups are close to each other than that of DCAs with a diamide-link chain length of two or four, which display slightly bent shapes (**1**, **3**, **4**, **6**, **7**, **9**, **10** and **12**).

In the dipole moment evaluation (Table 5), the calculated dipole moment of these compounds (**2**: 5.975 Debye, **5**: 5.248 Debye, **8**: 6.199 Debye, **11**: 6.335 Debye) showed a linear relationship for higher inhibitory activity with decreasing dipole moment (for inhibitory activity, **5** > **2** > **8** > **11**). Their diamide-link chin length is three. Their values of dipole moment were the lowest of DCAs with the same functional group and a diamide-link chain lengths of two or four. This relation is elucidated that the decrease in the dipole moment of DCAs increases tyrosinase inhibitory activity for possibility of binding to copper ions in the active cite of tyrosinase.

To compare the hydrophobic characteristics of DCAs, we calculated partition coefficient (Log *P*) values using Chemdraw program (Table 5). The hydrophobic characteristics were increased as the increase in diamide-link chain lengths and addition of a methoxy group. DCAs (**1**–**12**) indicated higher 1.5 of log *P* value, which increase in accessibility to the active site of tyroisnase and penetration into melanocytes. On the other hand, arbutin indicated very low log *P* value (-0.58) decreasing these abilities for depigmenting activity.

In the cell uptake evaluation (Fig. 4) of DCAs, compounds **3** and **6** showed the highest levels of cellular uptake and the lowest Log *P* values among the compounds having hydroxyl groups (–OH). Their cell uptake showed a correlation with log *P* indicating physical properties. However, the presence of –OH groups at the binding positions, R1 and R2, did not affect the cellular uptake of these compounds. Compounds 8 and 11 had a relatively low dipole moment and a diamide connection length of 3, and they showed the highest cellular uptake ratios within the group of compounds having both methoxy and hydroxyl groups (7–12).[33] Although the groups had low log *P* values, which was probably due to their highly hydrophilic nature, they showed higher cellular uptake ratios than the compounds with hydroxyl groups alone. These results suggest that the affinity between the methoxy group and the cell membrane leads to an increase in cellular uptake of DCAs. Arbutin, as a control, had a very low cellular uptake ratio due to its hydrophilic structure

Taken together, anti-melanogenic effects of DCAs are enhanced when their diamide-link chain length are three involving a folded shape, a low dipole moment, and appropriate hydrophobicity (> 1.5) and folded structure increase in accessibility to the active site of tyrosinase. Therefore, our results provide useful information for the design of dimeric compounds with antioxidant and whitening activities.

4. Conclusion

Dimeric compounds are widely developed to enhance the biological properties such as antioxidative and tyrosinase inhibitory activities. However, structure–activity relationship of dimeric compounds with regard to inhibitory effects on tyrosinase are not well known. In the present paper, DCAs (**1**–**12**) were synthesized to investigate the effect of functional groups and the diamide-link chain length in dimeric compounds. In detail, we adjusted two factors of the DCAs: 1) the position of the hydroxy and methoxy groups in the cinnamoyl group, 2) the diamide-link chain lengths (n = 2, 3, and 4) between the functional groups in the DCAs. In melanin production in α-MSH induced B16F1 cells, DCAs with the diamide-link chain length was three (**2**, **5**, **8** and **11**) only showed inhibitory effects. The compounds displayed folded structure and low dipole moments of DCAs with the same functional group. These characteristics of them are optimized to inhibit tyrosinase activity through copper-chelation as an active cite of tyrosinase. The results suggest that the diamide linkage chain length of DCAs is important to block the active site of tyrosinase, decreasing in melanin production effectively.

Recently, it has been reported that arbutin, 4-hexylresorcinol, and hydroquinone can be used as substrates for tyrosinase in the presence of hydrogen peroxide, ascorbic acid, or 4-*tert*-butylcatechol.[36–38] It has also been reported that the product of the reaction between hydroquinone and tyrosinase is toxic. Although the compounds we synthesized were not cytotoxic, the compounds also have phenolic groups similar to hydroquinone. Therefore, these compounds are likely to be converted by tyrosinase in the presence of hydrogen peroxide and various reducing agents, which may result in cytotoxicity. These issues will be thoroughly reviewed before future clinical studies on whitening effects.

In conclusion, these results provide a useful insight into the development of new dimeric compounds for various physiological active agents in the future. To understand the structure–activity relationship of dimeric compounds in the biological systems further detailed studies are required.

References

1. Slominski A, Tobin DJ, Shibahara S, Wortsman J. Melanin pigmentation in mammalian skin and its hormonal regulation. *Physiol Rev.* 2004;84:1155–1228.
2. Olivares C, Solano F. New insights into the active site structure and catalytic mechanism of tyrosinase and its related proteins. *Pigm Cell Melan Res.* 2009;22:750–760.
3. Costin GE, Hearing VJ. Human skin pigmentation: melanocytes modulate skin color in response to stress. *FASEB J.* 2007;21:976–994.
4. Parvez S, Kang M, Chung HS, et al. Survey and mechanism of skin depigmenting and lightening agents. *Phytother Res.* 2006;20:921–934.
5. Paramonov BA, Turkovskii II IL, Potokin NA, Chebotarev Yurlova VY. Photoprotective activity of melanin preparations in human skin exposed to UV irradiation: dependence on previous photoexposure. *Bull Exp Biol Med.*

2002;134:366–369.
6. Shin EM, Zhou HY, Xu GH, Lee SH, Merfort I, Kim YS. Anti-inflammatory activity of hispidol A 25-methyl ether, a triterpenoid isolated from Ponciri Immaturus Fructus. *Eur J Pharmacol.* 2010;627:318–324.
7. Yaar M, Wu C, Park HY, Panova I, Schutz G, Gilchrest BA. Bone morphogenetic protein-4, a novel modulator of melanogenesis. *J Biol Chem.* 2006;281:25307–25314.
8. Kim M, Shin S, Lee JA, Park D, Lee J, Jung E. Inhibition of melanogenesis by Gaillardia aristata flower extract. *BMC Compl Altern Med.* 2015;15:449.
9. Park HY, Kosmadaki M, Yaar M, Gilchrest BA. Cellular mechanisms regulating human melanogenesis. *Cell Mol Life Sci.* 2009;66:1493–1506.
10. Won YK, Lin CB, Seiberg M, et al. Galvanic zinc-copper microparticles inhibit melanogenesis via multiple pigmentary pathways. *Arch Dermatol Res.* 2014;306:27–35.
11. Romero-Graillet C, Aberdam E, Clement M, Ortonne JP, Ballotti R. Nitric oxide produced by ultraviolet-irradiated keratinocytes stimulates melanogenesis. *J Clin Invest.* 1997;99:635–642.
12. Novellino L, Napolitano A, Prota G. 5,6-Dihydroxyindoles in the fenton reaction: a model study of the role of melanin precursors in oxidative stress and hyperpigmentary processes. *Chem Res Toxicol.* 1999;12:985–992.
13. Ebanks JP, Wickett RR, Boissy RE. Mechanisms regulating skin pigmentation: the rise and fall of complexion coloration. *Int J Mol Sci.* 2009;10:4066–4087.
14. Ito S, Ojika M, Yamashita T, Wakamatsu K. Tyrosinase-catalyzed oxidation of rhododendrol produces 2-methylchromane-6,7-dione, the putative ultimate toxic metabolite: implications for melanocyte toxicity. *Pigm Cell Melan Res.* 2014;27:744–753.
15. Song K, An SM, Kim M, Koh JS, Boo YC. Comparison of the antimelanogenic effects of p-coumaric acid and its methyl ester and their skin permeabilities. *J Dermatol Sci.* 2011;63:17–22.
16. Shirota S, Miyazaki K, Aiyama R, Ichioka M, Yokokura T. Tyrosinase inhibitors from crude drugs. *Biol Pharm Bull.* 1994;17:266–269.
17. Mishima S, Inoh Y, Narita Y, et al. Identification of caffeoylquinic acid derivatives from Brazilian propolis as constituents involved in induction of granulocytic differentiation of HL-60 cells. *Bioorg Med Chem.* 2005;13:5814–5818.
18. Ortonne JP, Passeron T. Melanin pigmentary disorders: treatment update. *Dermatol Clin.* 2005;23:209–226.
19. Curto EV, Kwong C, Hermersdorfer H, et al. Inhibitors of mammalian melanocyte tyrosinase: in vitro comparisons of alkyl esters of gentisic acid with other putative inhibitors. *Biochem Pharmacol.* 1999;57:663–672.
20. Shin HJ, Oh CT, Kwon TR, et al. A novel adamantyl benzylbenzamide derivative, AP736, inhibits melanogenesis in B16F10 mouse melanoma cells via glycogen synthase kinase 3beta phosphorylation. *Int J Mol Med.* 2015;36:1353–1360.
21. Park SH, Kim DS, Kim WG, et al. Terrein: a new melanogenesis inhibitor and its mechanism. *Cell Mol Life Sci.* 2004;61:2878–2885.
22. Ha JH, Jeong YJ, Xuan SH, Lee JY, Park J, Park SN. Methyl-2-acetylamino-3-(4-hydroxyl-3,5-dimethoxybenzoylthio)propanoate suppresses melanogenesis through ERK signaling pathway mediated MITF proteasomal degradation. *J Dermatol Sci.* 2018.
23. Lo YH, Lin RD, Lin YP, Liu YL, Lee MH. Active constituents from Sophora japonica exhibiting cellular tyrosinase inhibition in human epidermal melanocytes. *J Ethnopharmacol.* 2009;124:625–629.
24. Choi SW, Lee SK, Kim EO, et al. Antioxidant and antimelanogenic activities of polyamine conjugates from corn bran and related hydroxycinnamic acids. *J Agric Food Chem.* 2007;55:3920–3925.
25. Criton M, Le Mellay-Hamon V. Dimeric cinnamoylamide derivatives as inhibitors of melanogenesis. *Biol Pharm Bull.* 2011;34:420–425.
26. Kim MK, Youk HS, Yoo JJ, et al. Synthesis of dimeric cinnamoylamide derivatives and evaluation of their depigmenting activities. *Bull Korean Chem Soc.* 2014;35:3085–3088.
27. Ha JH, Park SN. Mechanism underlying inhibitory effect of six dicaffeoylquinic acid isomers on melanogenesis and the computational molecular modeling studies. *Bioorg Med Chem.* 2018;26:4201–4208.
28. Maisuthisakul P, Gordon MH. Antioxidant and tyrosinase inhibitory activity of mango seed kernel by product. *Food Chem.* 2009;117:332–341.
29. Briganti S, Camera E, Picardo M. Chemical and instrumental approaches to treat hyperpigmentation. *Pigment Cell Res.* 2003;16:101–110.
30. Selinheimo E, NiEidhin D, Steffensen C, et al. Comparison of the characteristics of fungal and plant tyrosinases. *J Biotechnol.* 2007;130:471–480.
31. Hachinohe M, Matsumoto H. Involvement of reactive oxygen species generated from melanin synthesis pathway in phytotoxicty of L-DOPA. *J Chem Ecol.* 2005;31:237–246.
32. Park SN, Kim MJ, Ha JH, et al. Protective effects of TES trioleate, an inhibitor of phospholipase A2, on reactive oxygen species and UVA-induced cell damage. *J Photochem Photobiol B.* 2016;164:30–35.
33. Hwang JP, Ha JH, Kim MK, Park SN. Synthesis and antioxidative activities of N, N-diferuloyl-putrescine (DFP) and its derivatives. *Appl Chem Eng.* 2015;26:29–34.
34. Karamac M, Koleva L, Kancheva VD, Amarowicz R. The structure-antioxidant activity relationship of ferulates. *Molecules.* 2017;22.
35. Musa EM, Ali EO. Density functional theory (DFT) B3LYP study of antioxidant activity of 6-(2,2'-bithiophen-5yl) pyridine-3-carboximidamide, new model bichalcophenes derivatives. *J Appl Indust Sci.* 2015;3:126–132.
36. Garcia-Jimenez A, Teruel-Puche JA, Berna J, Rodriguez-Lopez JN, Tudela J, Garcia-Canovas F. Action of tyrosinase on alpha and beta-arbutin: a kinetic study. *PLoS ONE.* 2017;12.
37. Ortiz-Ruiz CV, Berna J, Rodriguez-Lopez JN, Tomas V, Garcia-Canovas FJ. Tyrosinase-catalyzed hydroxylation of 4-hexylresorcinol, an antibrowning and depigmenting agent: a kinetic study. *Agric Food Chem.* 2015;12:7032–7040.
38. Garcia-Molina M, Munoz Munoz JL, Martinez-Ortiz F, et al. Tyrosinase-catalyzed hydroxylation of hydroquinone, a depigmenting agent, to hydroxyhydroquinone: a kinetic study. *Bioorg Med Chem.* 2014;22:3360–3369.